Radiocarbon, Vol 56, Nr 1, 2014, p 127–141 DOI: 10.2458/56.16922

A CAVEAT ON RADIOCARBON DATING OF ORGANIC-POOR BULK LACUSTRINE SEDIMENTS IN ARID CHINA

Shi-Yong Yu[1,2,3] • Peng Cheng[1] • Zhanfang Hou[1]

ABSTRACT. Characterized by a dry climate, the arid area of China represents a unique landscape. A proper understanding of the driving mechanisms behind the changes of this ecologically vulnerable landscape requires placing the instrumental records within a geological context. Lakes in this area bear rich information about past climatic and environmental changes presumably regulated by the westerlies at various timescales. The lacustrine records obtained in this area heavily rely on radiocarbon ages, which are usually subject to the temporal and spatial variability of the ^{14}C reservoir effect. Yet, little is known about the ^{14}C reservoir age of lacustrine systems in this area. This study reports an anomalously large ^{14}C reservoir age of about 11,000 ± 2000 yr from a saline lake in NW China by comparing ^{14}C and OSL chronologies. The modeling study suggests that this age offset appears to be an inherent phenomenon in lacustrine systems, which mainly arises from the introduction of pre-aged organic matter from the catchment and the conversion of ^{14}C-depleted dissolved inorganic carbon to organic matter by photosynthesis. Compared to the large age offset induced by the ^{14}C-deficient exogenous carbon, the reservoir effect due to retention of organic matter in the lake water appears to be inconsequential. The results reveal the pitfall of ^{14}C dating on organic-poor bulk lacustrine sediments in this barren landscape, and thus highlight the need for alternate dating methods to constrain the chronology of lacustrine records.

INTRODUCTION

The landscape of arid China, characterized by deserts and sand fields formed under extremely dry and windy climate conditions (Yang et al. 2004), differs significantly from the monsoonal lowlands and the high, cold Tibetan Plateau. The increasing aridification within the context of global warming has imposed an adverse impact on human livelihood in this ecologically vulnerable zone (Yang et al. 2005). To better predict the trajectory of future environmental changes in this area, it is imperative to scrutinize geological records of past climate changes that cover a full range of variation (e.g. glacial-interglacial cycles). Lakes are exceptional archives of climatic and environmental changes towards this end. The past decade has seen the prosperity of paleolimnological studies in this area (An et al. 2006; Feng et al. 2006; Chen et al. 2008; Zhao et al. 2009). Lacustrine records derived from different proxies have substantially deepened our insight into the dynamics of the westerlies on a longer timescale. For example, synthesizing the existing lacustrine records in this area revealed an out-of-phase relationship of the westerlies with the Asian summer monsoon systems (Chen et al. 2008). Nevertheless, a precise timing of changes in these large physical systems over the Eurasian landmass is still hindered by the chronological uncertainty.

A reliable chronology is critical to paleoclimatic records, based on which the timing, magnitude, and rate of past climatic changes may be better defined. As a well-established method, ^{14}C dating has been intensively used to constrain the chronology of lacustrine records in this area (Chen et al. 1999, 2001, 2003, 2006; Zhang et al. 2000; Shi et al. 2002; Huang et al. 2009). However, the scarcity of terrestrial plant macrofossils and the low organic matter content in lake sediments of this area turn out to be the major hindrance towards determining a precise ^{14}C chronology of the lacustrine records (Zhang et al. 2006). ^{14}C ages on bulk organic matter from lakes in barren landscapes are known to be anomalously old (Pachur et al. 1995; Zhang et al. 2002, 2004). This is mainly caused by the introduction of pre-aged organic matter to the lake water, which in turn would result in a large deviation from the actual ^{14}C age known as the inheritance age. Prior to deposition, the organic matter may gain an additional age (i.e. residence age) while suspended in the lake water. These two apparent ages are collectively referred to as the ^{14}C reservoir age (Yu et al. 2007).

1. State Key Laboratory of Loess and Quaternary Geology, Institute of Earth Environment, CAS, Xi'an 710075, China.
2. Large Lakes Observatory, University of Minnesota Duluth, 2205 E. 5th Street, Duluth, Minnesota 55812, USA.
3. Corresponding author. Email: yusy@ieecas.cn; syu@d.umn.edu.

Previous studies revealed that lakes on the Tibetan Plateau commonly have a ^{14}C reservoir age, which varies from site to site and from time to time (Hou et al. 2012). The spatial and temporal uncertainties of this spurious age add another level of complexity to paleoclimatological studies in this area. Yet, little is known about the reservoir age of lakes in desert settings. This article presents evidence of anomalously large ^{14}C reservoir ages from Gaotai Lake, NW China, through a combination of ^{14}C and OSL dating. A one-box model of carbon cycling in lacustrine systems was developed to provide a theoretical perspective on this phenomenon. These modeling studies suggest that more attention should be paid when dating organic-poor bulk sediments in this arid area.

SITE DESCRIPTION AND STRATIGRAPHY

Gaotai Lake is located on the southern margin of the Badain Jaran Desert (Figure 1). The lake basin developed on a long (~16 km), narrow (~1.2 km) Cenozoic tectonic depression oriented in a nearly east-west direction (Figure 1). The bedrock of the catchments is mainly composed of Cretaceous sandstones and conglomerates. The surface area of the lake is ~18 km^2. There are no perennial rivers discharging to the lake, and the lake is mainly fed by precipitation and subsurface groundwater from the Hehe River. Characterized by temperate continental arid climate conditions, annual precipitation in this area is only 100 mm, most of which occurs in the summer, while annual evaporation is 2000 mm. Annual mean temperature is 7.6°C with a maximum temperature of 38°C occurring in July and a minimum temperature of −10°C occurring in January.

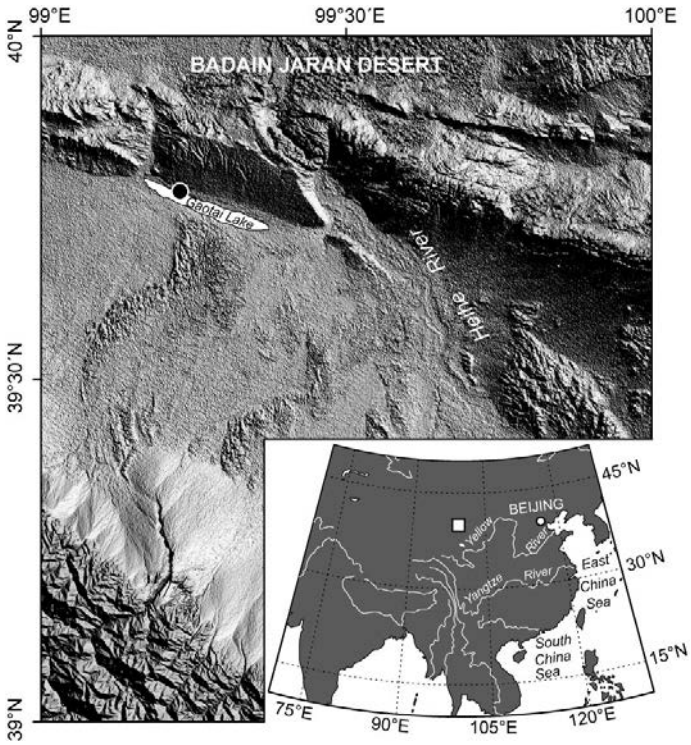

Figure 1 Map showing the location and topographical features of Gaotai Lake and the surrounding area in NW China. The filled circle indicates the location of the stratigraphical section studied.

The lake now is almost dried up due to extremely high evaporation, and most part of the lake bed is covered with silty Glauber's salt, gypsum, and halite. Fluvial fine sand and silty clay were deposited along the shore, forming the substrate of the first terrace, which is covered with fixed sand dunes. A continuous sediment sequence was recovered by excavating a trench on the north shore of the lake (39°46′42″N, 99′12′38″E). Four sedimentary units along the section can be identified (Figure 2).

Unit I (285–350 cm) is light-brown silt; Unit II (85–285 cm) is a thick layer of light-gray clay interbedded with silt; Unit III (15–85 cm) is dark-brown crossbedded fine sand deposited in a littoral environment; and Unit IV (0–15 cm) is modern sand dune composed of light-brown, massive fine sand.

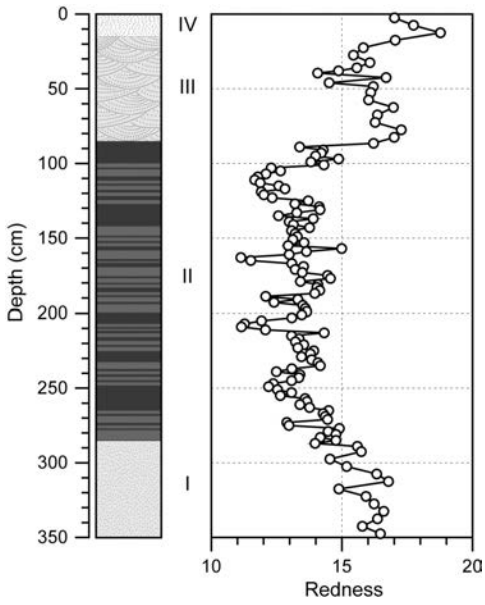

Figure 2 Diagram showing the changes in lithology and color (redness) as a function of depth in the Gaotai Lake, NW China.

METHODS

Sampling and Color Measurements

Samples for AMS ^{14}C dating were collected from selected clayey layers along a cleaned exposure of the trench, while those for optically stimulated luminescence (OSL) dating were taken by perpendicularly hammering a steel tube of ~20 cm in length and 2 cm in diameter into the silty layers at certain depths along the exposure. OSL samples were tightly sealed and warped with dark plastic film in the field for transportation to the laboratory. Samples were taken at 2–3 cm intervals along the exposure for color analyses, which were conducted using a Minolta CM-508i spectrophotometer in the State Key Laboratory of Loess and Quaternary Geology, CAS.

AMS Radiocarbon Dating

Subsamples of bulk organic matter were soaked in deionized water overnight, then transferred to an ultrasonic bath for 30 min to ensure a complete disintegration and homogenization. The wet samples were sieved using a 180-μm mesh to remove root fragments. To the samples 1M HCl was added, then samples were placed in a water bath at 70°C for 2 hr to dissolve carbonates. The samples were rinsed repeatedly until neutral, then dried overnight in an electric oven at 60°C. Finally, the desiccated samples were transferred into glass vials and sealed tightly for subsequent combustion and graphitization.

Subsamples of ~500 mg along with cuprous oxide were placed in a quartz tube and evacuated using a high-vacuum system. Once the vacuum level reached -1×10^{-5} Torr, the sample tube was isolated from the vacuum line. Samples were combusted at 800°C using a natural gas jet burner for ~20 min to ensure a thorough deliberation of CO_2 from different components of the bulk organic matter. The resulting gas was then passed through several cleaning elements to purify it. The purified CO_2 was

then collected using liquid nitrogen and reduced to graphite through Zn/Fe catalytic reduction. The residual radioactivity of the samples with respect to that of the modern ^{14}C standard was measured in the Xi'an AMS Center, CAS. Chinese sugar beet carbon was used as a secondary ^{14}C standard, which in turn was converted to the international modern ^{14}C standard for calculation of ^{14}C ages (Stuiver and Polach 1977).

OSL Dating

Given the setting of the lake and organic-poor nature of the lacustrine sediments, an independent chronological framework of the sediment sequence was constructed by dating fine-grained quartz using the recuperated optically stimulated luminescence (ReOSL) dating method and following the multiple-aliquot regenerative-dose (MAR) approach (Wang et al. 2006b). Pretreatments and luminescence measurements of the samples were conducted in the State Key Laboratory of Loess and Quaternary Geology, CAS. Although there have been several potential problems with the MAR protocol (e.g. the heterogeneous ages of subsamples and partial bleaching in quartz), the OSL method has great potential to directly date the organic-poor lacustrine sediments in a desert setting.

Due to the potential exposure to daylight while sampling, sediments for quartz equivalent dose (D_E) determination were only taken from the middle part of each steel tube under subdued red-light conditions, while sediments at the two ends of each steel tube were used for radioisotope (U, Th, and K) measurements of concentration. The fine-grained (4–11 μm) quartz grains were extracted following the procedures as described in Wang et al. (2006a) and Lu et al. (2007). Samples of approximately 50 g were first treated with 30% H_2O_2 and 30% HCl to remove organic matter and carbonates, respectively. After the solution was washed with distilled water until neutral, the 4–11 μm polymineral grains were separated, and then they were soaked in 30% hydrofluorosilicic (H_2SiF_6) for 3–5 days in an ultrasonic bath to allow the extraction of the fine-grained quartz. Purified quartz grains were transferred to a stainless steel disk of 9.7 mm in diameter for experiments.

The purity of the isolated quartz was checked by regenerative dose infrared (IR) stimulation. All the measurements were carried out using an automated Daybreak 2200 OSL reader equipped with infrared (880 ± 60 nm) and blue (470 ± 5 nm) LED units and a $^{90}Sr/^{90}Y$ beta source (0.14 Gy/s) for irradiation. The quartz OSL signal was stimulated at 125°C with blue LEDs and detected through an EMI 9235QA photomultiplier tube coupled in front with two U-340 (290–370 nm) glass filters. For D_E determination, the net OSL signal was calculated using the integral of first 5 s of the OSL decay curve subtracted with that of the last 5 s.

One-Box Model of Lacustrine Carbon Cycling

To better understand the ^{14}C reservoir effect in lacustrine systems, a one-box model of carbon cycling in the lake water was established based on mass conservation. This is a simplified version of the model put forward by Yu et al. (2007) without considering early diagenesis. In this one-box model, the lake-water column is treated as a homogeneous carbon pool. Autochthonous organic carbon in the lake water is assumed to be of totally atmospheric origin. Note that the aquatic photosynthesis may use dissolved inorganic carbon partly derived from the weathering of catchment bedrock (e.g. carbonate) that could be greatly depleted in ^{14}C (Yu et al. 2007). But this assumption is absolutely valid for lakes with a catchment of silicate bedrock. Catchment input through eolian and/or fluvial processes represents the major source of allochthonous organic carbon, which could be pre-aged. The molar mass of organic carbon input to the lake water is balanced by deposition and decomposition as well as the decay of ^{14}C (Figure 3).

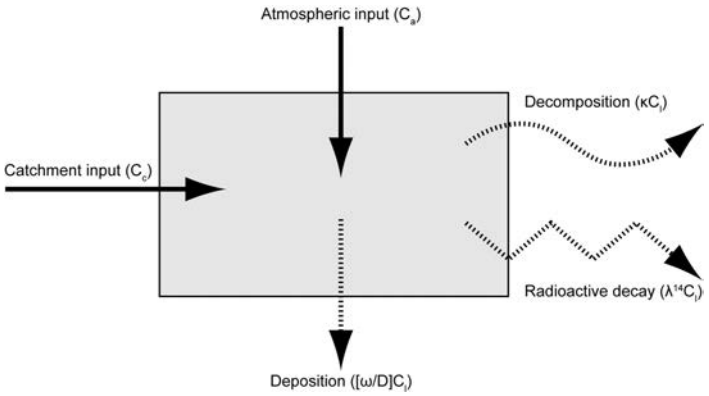

Figure 3 Schematic diagram of one-box model of organic carbon cycling in lacustrine systems.

Specifically, the molar mass balance of ^{12}C and ^{14}C in the lake carbon pool can be written as

$$\frac{\partial {}^{12}C_l}{\partial t} = {}^{12}C_a + {}^{12}C_c - \left(\kappa + \frac{\omega}{D}\right){}^{12}C_l \tag{1}$$

$$\frac{\partial {}^{14}C_l}{\partial t} = {}^{14}C_a + {}^{14}C_c - \left(\kappa + \frac{\omega}{D} + \lambda\right){}^{14}C_l \tag{2}$$

where C_l = dissolved organic carbon in lake water; C_a = atmospheric input through primary productivity; C_c = catchment input through fluvial and/or eolian processes; D = lake water depth; κ = decomposition rate of organic carbon; ω = sedimentation rate; and λ = decay constant of ^{14}C (λ = 1/8033 yr^{-1} derived from the 5568-yr half-life)

The solutions to Equations 1 and 2 are thus

$${}^{12}C_l = \frac{{}^{12}C_a + {}^{12}C_c}{\kappa + \frac{\omega}{D}}\left[1 - e^{-\left(\kappa + \frac{\omega}{D}\right)t}\right] \tag{3}$$

$${}^{14}C_l = \frac{{}^{14}C_a + {}^{14}C_c}{\kappa + \frac{\omega}{D} + \lambda}\left[1 - e^{-\left(\kappa + \frac{\omega}{D} + \lambda\right)t}\right] \tag{4}$$

At steady state, the solution turns out to be

$${}^{12}C_l = \frac{{}^{12}C_a + {}^{12}C_c}{\kappa + \frac{\omega}{D}} \tag{5}$$

$${}^{14}C_l = \frac{{}^{14}C_a + {}^{14}C_c}{\kappa + \frac{\omega}{D} + \lambda} \tag{6}$$

Therefore, the radioactivity of organic carbon in the lake water can be expressed as

$$A_l = \frac{{}^{14}C_l}{{}^{12}C_l} = \frac{\kappa + \frac{\omega}{D}}{\kappa + \frac{\omega}{D} + \lambda} \times \frac{{}^{14}C_a + {}^{14}C_c}{{}^{12}C_a + {}^{12}C_c} \tag{7}$$

Normalizing A_l for the isotope fractionation leads to

$$A_{lN} = A_l\left[1-\frac{2\left(25+\delta^{13}C_l\right)}{1000}\right] \tag{8}$$

The radioactive decay follows the exponential law

$$A_{lN} = A_{ON}e^{\lambda t} \tag{9}$$

where A_{ON} is the radioactivity (i.e. $^{14}C/^{12}C$) of the oxalic acid standard normalized for isotope fractionation (Stuiver and Polach 1977). Solving for t and substituting $^{12}C_a$, $^{12}C_c$, $^{14}C_a$, and $^{14}C_c$ with that given in Equations A11–14 (in Appendix), respectively, yields the conventional ^{14}C age in terms of years before 1950 (van der Plicht and Hogg 2006)

$$t = -\frac{1}{\lambda}\ln\left\{\frac{\kappa+\frac{\omega}{D}}{\kappa+\frac{\omega}{D}+\lambda}\times\frac{\frac{\left(\frac{d^{14}C_a}{1000}+1\right)C_a}{1+\left(\frac{\delta^{13}C_a}{1000}+1\right)R_{PDB}}+\frac{\left(\frac{d^{14}C_c}{1000}+1\right)C_c}{1+\left(\frac{\delta^{13}C_c}{1000}+1\right)R_{PDB}}}{\frac{C_a}{1+\left(\frac{\delta^{13}C_a}{1000}+1\right)R_{PDB}}+\frac{C_c}{1+\left(\frac{\delta^{13}C_c}{1000}+1\right)R_{PDB}}}\times\left[1-\frac{2\left(25+\delta^{13}C_l\right)}{1000}\right]\right\} \tag{10}$$

It is reasonable to assume that $\delta^{13}C_a = \delta^{13}C_c = \delta^{13}C_l$, thereby leading to a simplified expression of the above equation

$$t = -\frac{1}{\lambda}\ln\left\{\frac{\kappa+\frac{\omega}{D}}{\kappa+\frac{\omega}{D}+\lambda}\times\frac{\left(\frac{d^{14}C_a}{1000}+1\right)C_a+\left(\frac{d^{14}C_c}{1000}+1\right)C_c}{C_a+C_c}\times\left[1-\frac{2\left(25+\delta^{13}C_l\right)}{1000}\right]\right\} \tag{11}$$

For the sake of discussion, it is better to relate the notation of per mil in the above equation to percent modern carbon (pMC). Making use of the relationship given in Equations A23–24 (in Appendix) gives

$$t = -\frac{1}{\lambda}\ln\left[\frac{\kappa+\frac{\omega}{D}}{\kappa+\frac{\omega}{D}+\lambda}\times\frac{\frac{pMC_a}{100}C_a+\frac{pMC_c}{100}C_c}{C_a+C_c}\right]-\frac{\lambda^*}{\lambda}\left(y-1950\right) \tag{12}$$

Equation 12 reveals that the ^{14}C age of the lake water arises from three components: (1) the retention of organic carbon in the lake water, which may lead to an apparent age (the residence age); (2) the atmospheric and catchment input of organic carbon to the lake water, the former representing the actual age, while the latter may result in a spurious age (the inheritance age); and (3) an age correction if the measurement was not made in 1950.

RESULTS

A total of 12 ^{14}C and 5 OSL ages were obtained. Detailed results are presented in Tables 1 and 2. All of the ^{14}C ages appear to be anomalously old (>9000 yr BP), and they exhibit a large scattering along depth (Figure 4A). In contrast to the ^{14}C ages, the OSL ages are relatively more stratigraph-

ically consistent, and they are well ordered along depth, albeit with only one reversal (Figure 4B). The age-depth relationship can be best fit using a linear model, revealing a nearly constant sedimentation rate of ~0.5 mm/yr during the last 8000 yr. Note that this regression analysis is based on the entire data set including the aberrant result at 286–288 cm. A large deviation of this point from the age-depth model confirms it being an outlier. Although this small data set may be less adequate to define a linear age-depth model, the large coefficient of determination ($R^2 = 0.98$) suggests that this appears to be a satisfactory expedient.

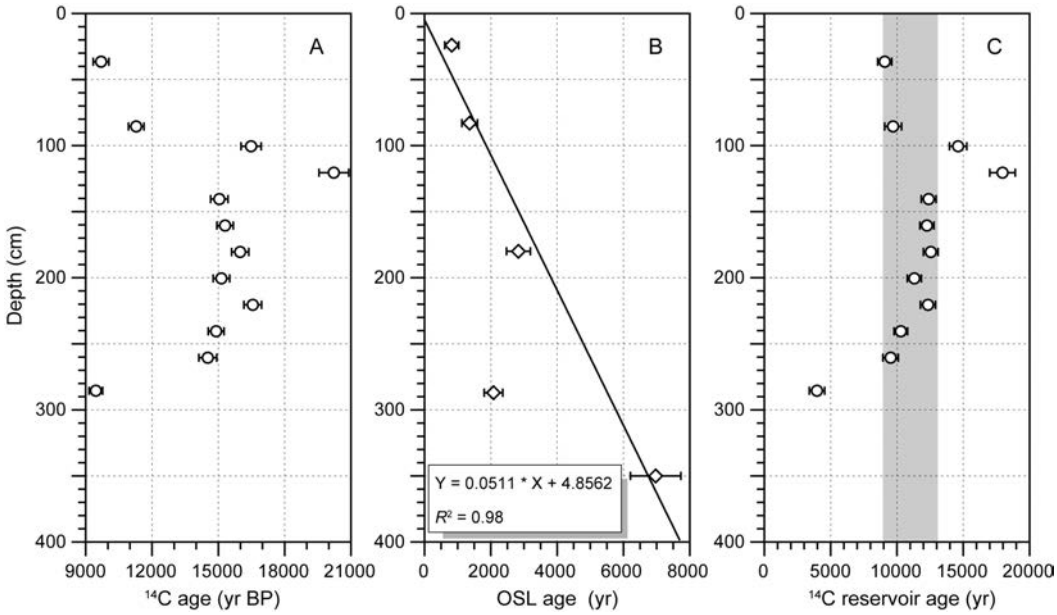

Figure 4 (A) Biplot of ^{14}C ages versus depths; (B) biplot of OSL ages versus depths; (C) changes in ^{14}C reservoir ages obtained by comparing the ^{14}C and OSL chronologies.

Table 1 Radiocarbon ages of Gaotai Lake, NW China.

Lab nr	Depth (cm)	Material dated	$\delta^{13}C$ (‰ VPDB)	C yield (%)	^{14}C age (yr BP)	2σ calibrated age (yr BP)
XA6660	36−37	Bulk organic matter	−20.9	0.09	9695 ± 40	10,870−11,220
XA6659	85−86	Bulk organic matter	−22.7	0.09	11,280 ± 50	13,090−13,300
XA6633	100−101	Bulk organic matter	−24.9	0.20	16,480 ± 65	19,420−13,300
XA6632	120−121	Bulk organic matter	−26.3	0.21	20,225 ± 95	23,850−24,440
XA6625	140−141	Bulk organic matter	−23.8	0.18	15,045 ± 55	18,020−18,550
XA6630	160−161	Bulk organic matter	−24.7	0.24	15,305 ± 50	18,200−18,720
XA6626	180−181	Bulk organic matter	−24.5	0.23	15,985 ± 55	18,910−19,400
XA6628	200−201	Bulk organic matter	−24.3	0.25	15,135 ± 55	18,030−18,610
XA6631	220−221	Bulk organic matter	−24.6	0.25	16,560 ± 55	19,450−20,010
XA6634	240−241	Bulk organic matter	−23.4	0.26	14,900 ± 50	17,900−18,520
XA6627	260−261	Bulk organic matter	−26.0	0.24	14,520 ± 60	17,260−17,940
XA6635	285−286	Bulk organic matter	−23.4	0.16	9455 ± 45	10,570−11,060

^{14}C reservoir ages for this lake could be estimated by comparing the observed ^{14}C and OSL ages, if the latter were assumed to represent the actual ages of the stratigraphy. However, the observed ^{14}C and OSL ages are not paired. A linear OSL age-depth model was used to determine the actual ^{14}C ages of the given depths. Subtracting the modeled ages from the observed ^{14}C ages yields large and time-varying ^{14}C reservoir ages (Figure 4C). Most of the reservoir ages lie between 9000 and 13,000 yr, probably indicating a constant source from which substantially ^{14}C-depleted organic carbon was exported to the lake with episodic storms and/or floods.

Table 2 OSL ages of Gaotai Lake, NW China.

Lab nr	Depth (cm)	U (ppm)	Th (ppm)	K (%)	Water content (%)	Dose rate (Gy/ka)	Equivalent dose (Gy)	Age (kyr)
IEE3606	23−25	1.40	7.49	1.51	15 ± 5	2.77 ± 0.14	2.26 ± 0.08	0.82 ± 0.05
IEE3607	82−84	4.62	7.71	1.57	15 ± 5	3.80 ± 0.25	5.16 ± 0.07	1.36 ± 0.09
IEE3608	179−181	3.41	13.78	2.32	15 ± 5	4.59 ± 0.26	12.98 ± 0.41	2.83 ± 0.18
IEE3609	286−288	2.93	8.35	1.59	15 ± 5	3.27 ± 0.21	6.80 ± 0.11	2.08 ± 0.14
IEE3610	349−351	1.98	6.00	1.72	15 ± 5	2.88 ± 0.15	20.07 ± 0.29	6.97 ± 0.38

DISCUSSION

Spatiotemporal Variability of Radiocarbon Reservoir Age

The ^{14}C reservoir effect appears to be a pervasive phenomenon for lakes situated on a barren landscape. For example, ^{14}C dating of bulk organic matter of sediment cores from lakes across the high, cold Tibetan Plateau and extrapolating the age-depth models to the core top yield apparent ages of 1000–3000 yr (Fontes et al. 1993; Herzschuh et al. 2006; Wu et al. 2006, 2010; Liu et al. 2008; Mischke and Zhang 2010; Opitz et al. 2012; Mischke et al. 2013), presumably representing the ^{14}C reservoir ages. The reservoir ages are site specific and thus exhibit a large spatial variability in this area (Hou et al. 2012), varying from 650 yr at Ahung Co (Morrill et al. 2006) to 6670 yr at Bangong Co (Fontes et al. 1996). This spatial variability, to the most extent, depends on localized hydrological and geological conditions.

The reservoir age also tends to vary from time to time. There are several methods that have been used to determine the changes in the reservoir ages. These methods include (1) comparison between ^{14}C ages and modeled ages based on sedimentation rate determined by short-lived radioactive nuclides (Zhu et al. 2008; Liu et al. 2009); (2) comparison of ^{14}C ages on different factions, e.g. bulk organic carbon vs. lignin phenols (Hou et al. 2010) or alkali-insoluble versus -soluble fractions (Mischke et al. 2010); (3) geochemical modeling (Wang et al. 2007); and (4) comparison between ^{14}C and varve chronologies (Zhou et al. 2011). Each method has its own advantages and limitations. A detailed discussion of these methods is beyond the scope of this study.

A combination of ^{14}C and OSL dating on bulk organic matter and fine-grained quartz fractions, respectively, appears to be a promising method for determining the temporal variability of reservoir ages for lakes situated in a desert setting. For example, the ^{14}C and OSL ages exhibit a significant difference along a sediment sequence at Lop Nur in the Tarim Basin (Zhang et al. 2012), implying a large and time-varying ^{14}C reservoir age that is comparable with that revealed in this study (about 11,000 ± 2000 yr). However, applying this method onto the Qingtu Lake on the northwestern margin of the Tengger Desert revealed a negligible reservoir age (Long et al. 2011). This might be an isolated case. In the following sections, a one-box model of lacustrine carbon cycling will be used to demonstrate that (1) the reservoir effect is an intrinsic phenomenon in lacustrine systems due to the retention of organic carbon in the lake water prior to burial (i.e. the residence age) and (2) the

reservoir age could be anomalously large, depending on the extent to which the reworked organic carbon was depleted in ^{14}C while resting in the catchment (i.e. the inheritance age).

Residence Age

The residence age is a kind of reservoir age resulting from radioactive decay while the organic matter resided in the lake water. Following Equation 12, this component is defined as

$$T_r = -\frac{1}{\lambda}\ln\left[\frac{\kappa + \frac{\omega}{D}}{\kappa + \frac{\omega}{D} + \lambda}\right] \tag{13}$$

The residence of ^{14}C in the lake water may cause a varying deviation from the actual age (Stein et al. 2004), depending on several factors such as the decomposition rate (κ), sedimentation rate (ω), and water depth (D). This apparent age is ubiquitous and inevitable in the lacustrine system, because it would not vanish unless either κ or ω or both approach infinite (i.e. κ, $\omega \rightarrow \infty$). To probe into the dependence of the residence age on these variables, a modeling study was conducted. Three types of lakes were considered according to water depth: (1) shallow lakes (D = 2 m); (2) intermediate lakes (D = 20 m); and (3) deep lakes (D = 200 m). The residence age, T_r, varies significantly for lakes of different water depths (Figure 5). For shallow lakes, T_r exhibits a strong dependence on both κ and ω, which are equally important. The residence age decreases rapidly as both variables increase (Figure 5A). For shallow lakes, as sedimentation rate is commonly high and the lake water can be quickly replenished, the residence age (usually <200 yr) is negligible. However, for intermediate depth lakes, T_r depends more on κ than on ω, which tends to decrease rapidly as κ increases (Figure 5B). For this kind of lake, a residence age of 200−400 yr prevails. For deep lakes, T_r appears to be a function of only κ (Figure 5C). This "stratification" represents the long residence age, which may lead to a reservoir age as large as l000 yr.

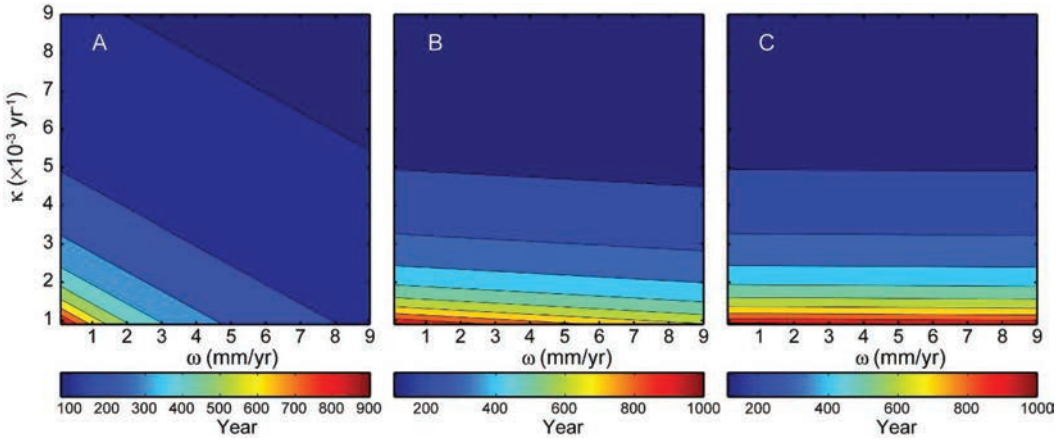

Figure 5 Modeled residence age as a function of the decomposition rate of organic carbon and sedimentation rate for lakes of different water depths: (A) shallow lakes (D = 2 m); (B) intermediate lakes (D = 20 m); (C) deep lakes (D = 200 m).

Inheritance Age

The inheritance age represents another kind of reservoir effect gained from the pre-aged organic matter introduced to the lake. According to Equation 12, this apparent age can be simply defined as

$$T_i = -\frac{1}{\lambda}\ln\left[\frac{\kappa+\frac{\omega}{D}}{\kappa+\frac{\omega}{D}+\lambda}\times\frac{\frac{pMC_a}{100}C_a+\frac{pMC_c}{100}C_c}{C_a+C_c}\right]+\frac{1}{\lambda}\ln\left[\frac{\kappa+\frac{\omega}{D}}{\kappa+\frac{\omega}{D}+\lambda}\times\frac{pMC_a}{100}\right]$$

$$=-\frac{1}{\lambda}\ln\left[\frac{1+\frac{pMC_c}{pMC_a}\frac{C_c}{C_a}}{1+\frac{C_c}{C_a}}\right] \quad (14)$$

This age could be anomalously old compared to the actual age, depending on the ratio of the ^{14}C-depleted allochthonous organic carbon to the autochthonous organic carbon of contemporaneously atmospheric origin. A modeling study was conducted to investigate this issue. Two scenarios were considered: (1) lakes dominated by autochthonous organic carbon (i.e. C_c/C_a <1) and (2) lakes dominated by allochthonous organic carbon (i.e. C_c/C_a >1). The first case may represent lakes in temperate and tropical areas where the primary productivity is high. For this kind of lake, the inheritance age, T_i, depends on both the radioactivity and influx of the allochthonous organic carbon relative to those of the autochthonous organic carbon (Figure 6A). T_i could be small (<500 yr) if the ratio of the radioactivity of the allochthonous organic carbon to that of the autochthonous organic carbon (pMC_c/pMC_a) was >0.85 or the ratio of the influx of the allochthonous organic carbon to that of the autochthonous organic carbon (C_c/C_a) was <0.1. T_i would vanish if the organic carbon input to the lake was of totally atmospheric origin (i.e. $C_c/C_a = 1$). T_i could be as old as ~5000 yr if nearly the same amount (i.e. $C_c/C_a = 1$) of extremely ^{14}C-deficient organic carbon (e.g. $pMC_c/pMC_a < 0.1$) as those derived from the concurrent atmospheric CO_2 was input to the lake.

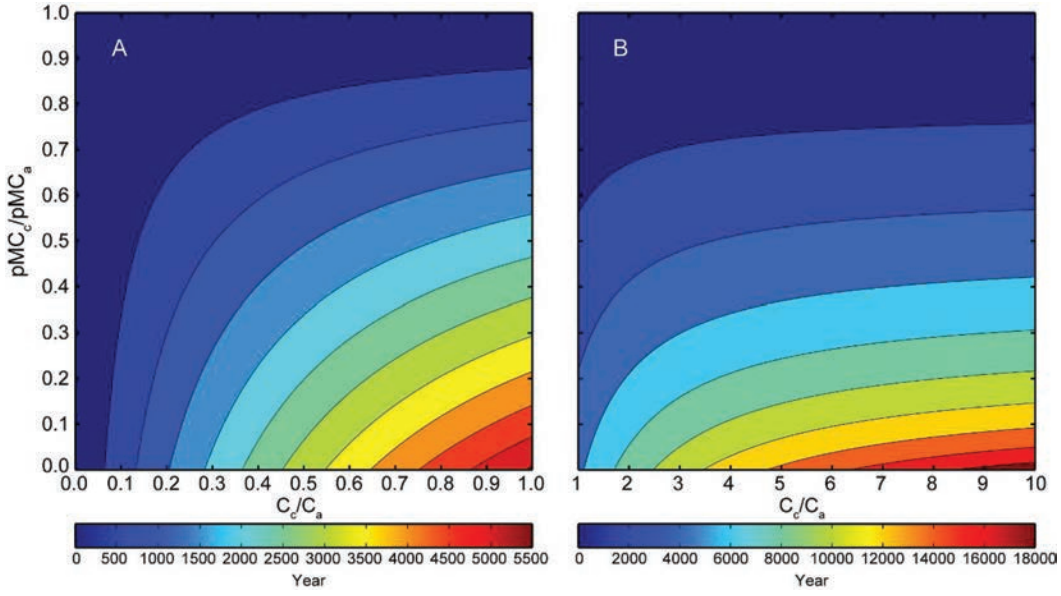

Figure 6 Modeled inheritance age as a function of the activity and influx of the ^{14}C-depleted allochthonous organic carbon relative to those of the autochthonous organic carbon of contemporaneously atmospheric origin: (A) lakes dominated by autochthonous organic carbon ($C_c/C_a < 1$); (B) lakes dominated by allochthonous organic carbon ($C_c/C_a > 1$).

In contrast to lakes with high productivity, the second case represents lakes situated in cold and arid areas where the primary productivity is extremely low. This is the case for the lake studied here. Regardless of the fraction of ^{14}C-deficient organic carbon in the lake carbon pool, an inheritance age of ~2000 yr prevails when $pMC_c/pMC_a > 0.7$ (Figure 6B). This may explain the reservoir effect of lakes across the Tibetan Plateau (Hou et al. 2012; Mischke et al. 2013). The inheritance age tends to get old as pMC_c/pMC_a decreases and C_c/C_a increases, and an anomalously old age of ~15,000 yr could occur if much more (e.g. $C_c/C_a > 8$) extremely ^{14}C-deficient organic carbon (e.g. $pMC_c/pMC_a < 0.1$) than that of contemporaneously atmospheric origin was input to the lake. The reservoir age of ~11,000 ± 2000 yr in Gaotai Lake suggests that at least threefold more ^{14}C-deficient organic carbon ($0.1 < pMC_c/pMC_a < 0.3$) than that of atmospheric origin was input to this lake via eolian or fluvial processes during the last 8000 yr.

CONCLUSIONS

A combination of ^{14}C and OSL dating on lacustrine sediments from Gaotai Lake, NW China, reveals an extremely large ^{14}C reservoir age of about 11,000 ± 2000 yr. This modeling study suggests that the ^{14}C reservoir effect associated with the introduction and retention of pre-aged organic carbon as well as the decay of ^{14}C in the water column is an inherent phenomenon in many lacustrine systems. The reservoir age could be anomalously old, depending on not only the fraction, but also the radioactivity of the ^{14}C-deficient exogenous organic matter relative to the endogenous organic carbon of contemporaneously atmospheric origin. Therefore, more attention should be paid when conducting ^{14}C dating of organic-poor bulk lacustrine sediments in this area.

The problem surrounding ^{14}C dating of organic-poor bulk lacustrine sediments in arid Chinese settings highlights the need for an alternate dating method. Given that the lacustrine sediments in the desert setting are mainly derived from the catchment through episodic storm and/or flood entrainments, the luminescence signals might have been reset during the transportation processes prior to burial in the lake. Therefore, the OSL method, particularly when implemented in conjunction with the single-aliquot regenerative-dose (SAR) protocol, may relax the limitations of ^{14}C dating on organic-poor lacustrine sediments in this setting, standing out as a promising method for constraining the chronology of lacustrine records.

ACKNOWLEDGMENTS

This work was supported by the Strategic Priority Research Program (Grant No. XDA05120401), the National Basic Research Program of China (No: 2013CB955903), and the "100-Talents" Program of the Chinese Academy of Sciences. We thank Xiangzhong Li, Jianghu Lan, and Tian Feng for their assistance during fieldwork. Our gratitude is also extended to Prof A J Timothy Jull and an anonymous reviewer for their insightful comments on the manuscript.

REFERENCES

An C-B, Feng Z-D, Barton L. 2006. Dry or humid? Mid-Holocene humidity changes in arid and semi-arid China. *Quaternary Science Reviews* 25(3):351–61.

Chen F, Shi Q, Wang J-M. 1999. Environmental changes documented by sedimentation of Lake Yiema in arid China since the Late Glaciation. *Journal of Paleolimnology* 22(2):159–69.

Chen F, Zhu Y, Li J, Shi Q, Jin L, Wünemann B. 2001. Abrupt Holocene changes of the Asian monsoon at millennial- and centennial-scales: evidence from lake sediment document in Minqin Basin, NW China. *Chinese Science Bulletin* 46(23):1942–7.

Chen F, Wu W, Holmes J, Madsen D, Zhu Y, Jin M, Oviatt C. 2003. A mid-Holocene drought interval as evidenced by lake desiccation in the Alashan Plateau, Inner Mongolia China. *Chinese Science Bulletin* 48(14):1401–10.

Chen F, Cheng B, Zhao Y, Zhu Y, Madsen DB. 2006. Holocene environmental change inferred from a high-resolution pollen record, Lake Zhuyeze, arid China. *The Holocene* 16(5):675–84.

Chen F, Yu Z, Yang M, Ito E, Wang S, Madsen DB, Huang X, Zhao Y, Sato T, Birks JB, Boomer I, Chen J, An CB, Wünnemann B. 2008. Holocene moisture evolution in arid central Asia and its out-of-phase relationship with Asian monsoon history. *Quaternary Science Reviews* 27(3):351–64.

Feng Z-D, An C, Wang H. 2006. Holocene climatic and environmental changes in the arid and semi-arid areas of China: a review. *The Holocene* 16(1):119–30.

Fontes J-C, Melieres F, Gibert E, Qing L, Gasse F. 1993. Stable isotope and radiocarbon balances of two Tibetan lakes (Sumxi Co, Longmu Co) from 13,000 BP. *Quaternary Science Reviews* 12(10):875–87.

Fontes J-C, Gasse F, Gibert E. 1996. Holocene environmental changes in Lake Bangong basin (Western Tibet). Part 1: Chronology and stable isotopes of carbonates of a Holocene lacustrine core. *Palaeogeography, Palaeoclomatology, Palaeoecology* 120(1):25–47.

Herzschuh U, Winter K, Wünnemann B, Li S. 2006. A general cooling trend on the central Tibetan Plateau throughout the Holocene recorded by the Lake Zigetang pollen spectra. *Quaternary International* 154–155:113–21.

Hou J, Huang Y, Brodsky C, Alexandre MR, McNichol AP, King JW, Hu FS, Shen J. 2010. Radiocarbon dating of individual lignin phenols: a new approach for establishing chronology of late Quaternary lake sediments. *Analytical Chemistry* 82(17):7119–26.

Hou J, D'Andrea WJ, Liu Z. 2012. The influence of ^{14}C reservoir age on interpretation of paleolimnological records from the Tibetan Plateau. *Quaternary Science Reviews* 48:67–79.

Huang X, Chen F, Fan Y, Yang M. 2009. Dry late-glacial and early Holocene climate in arid central Asia indicated by lithological and palynological evidence from Bosten Lake, China. *Quaternary International* 194(1):19–27.

Liu X, Dong H, Rech JA, Matsumoto R, Yang B, Wang Y. 2008. Evolution of Chaka Salt Lake in NW China in response to climatic change during the Latest Pleistocene–Holocene. *Quaternary Science Reviews* 27(7–8):867–79.

Liu X, Dong H, Yang X, Herzschuh U, Zhang E, Stuut J-BW, Wang Y. 2009. Late Holocene forcing of the Asian winter and summer monsoon as evidenced by proxy records from the northern Qinghai–Tibetan Plateau. *Earth and Planetary Science Letters* 280(1–4):276–84.

Long H, Lai Z, Wang N, Zhang J. 2011. A combined luminescence and radiocarbon dating study of Holocene lacustrine sediments from arid northern China. *Quaternary Geochronology* 6(1):1–9.

Lu Y, Wang X, Wintle AG. 2007. A new OSL chronology for dust accumulation in the last 130,000 yr for the Chinese Loess Plateau. *Quaternary Research* 67(1):152–60.

Mischke S, Zhang C. 2010. Holocene cold events on the Tibetan Plateau. *Global and Planetary Change* 72(3):155–63.

Mischke S, Zhang C, Börner A, Herzschuh U. 2010. Lateglacial and Holocene variation in aeolian sediment flux over the northeastern Tibetan Plateau recorded by laminated sediments of a saline meromictic lake. *Journal of Quaternary Science* 25(2):162–77.

Mischke S, Weynell M, Zhang C, Wiechert U. 2013. Spatial variability of ^{14}C reservoir effects in Tibetan Plateau lakes. *Quaternary International* 313–314:147–55.

Morrill C, Overpeck JT, Cole JE, Liu K-B, Shen C, Tang L. 2006. Holocene variations in the Asian monsoon inferred from the geochemistry of lake sediments in central Tibet. *Quaternary Research* 65(2):232–43.

Opitz S, Wünnemann B, Aichner B, Dietze E, Hartmann K, Herzschuh U, Ijmker J, Lehmkuhl F, Li S, Mischke S, Plotzki A, Stauch G, Diekmann B. 2012. Late Glacial and Holocene development of Lake Donggi Cona, north-eastern Tibetan Plateau, inferred from sedimentological analysis. *Palaeogeography, Palaeoclimatology, Palaeoecology* 337–338:159–76.

Pachur H-J, Wünnemann B, Zhang H. 1995. Lake evolution in the Tengger Desert, Northwestern China, during the last 40,000 years. *Quaternary Research* 44(2):171–80.

Shi Q, Chen F-H, Zhu Y, Madsen D. 2002. Lake evolution of the terminal area of Shiyang River drainage in arid China since the last glaciation. *Quaternary International* 93–94:31–43.

Stein M, Migowski C, Bookman R, Lazar B. 2004. Temporal changes in radiocarbon reservoir age in the Dead Sea-Lake Lisan system. *Radiocarbon* 46(2):649–55.

Stuiver M, Polach HA. 1977. Discussion: reporting of ^{14}C data. *Radiocarbon* 19(3):355–63.

van der Plicht J, Hogg A. 2006. A note on reporting radiocarbon. *Quaternary Geochronology* 1(4):237–40.

Wang X, Lu Y, Zhao H. 2006a. On the performances of the single-aliquot regenerative-dose (SAR) protocol for Chinese loess: fine quartz and polymineral grains. *Radiation Measurements* 41(1):1–8.

Wang X, Lu Y, Wintle A. 2006b. Recuperated OSL dating of fine-grained quartz in Chinese loess. *Quaternary Geochronology* 1(2):89–100.

Wang Y, Shen J, Wu J-L, Liu X-Q, Zhang E-L, Liu E-F. 2007. Hard-water effect correction of lacustrine sediment ages using the relationship between ^{14}C levels in lake waters and in the atmosphere: the case of Lake Qinghai. *Journal of Lake Sciences* 19:504–8 In Chinese with English abstract.

Wu Y, Lücke A, Jin Z, Wang S, Schleser GH, Battarbee RW, Xia W. 2006. Holocene climate development on the central Tibetan Plateau: a sedimentary record from Cuoe Lake. *Palaeogeography, Palaeoclimatology, Palaeoecology* 234(2–4):328–40.

Wu Y, Li S, Lücke A, Wünnemann B, Zhou L, Reimer P, Wang S. 2010. Lacustrine radiocarbon reservoir ages in Co Ngoin and Zigê Tangco, central Tibetan

Plateau. *Quaternary International* 212(1):21–5.
Yang X, Rost KT, Lehmkuhl F, Zhenda Z, Dodson J. 2004. The evolution of dry lands in northern China and in the Republic of Mongolia since the Last Glacial Maximum. *Quaternary International* 118–119:69–85.
Yang X, Zhang K, Jia B, Ci L. 2005. Desertification assessment in China: An overview. *Journal of Arid Environments* 63(2):517–31.
Yu S-Y, Shen J, Colman SM. 2007. Modeling the radiocarbon reservoir effect in lacustrine systems. *Radiocarbon* 49(3):1241–54.
Zhang H, Ma Y, Wünnemann B, Pachur H-J. 2000. A Holocene climatic record from arid northwestern China. *Palaeogeography, Palaeoclimatology, Palaeoecology* 162(3):389–401.
Zhang H, Wünnemann B, Ma Y, Peng J, Pachur H-J, Li J, Qi Y, Chen G, Fang H, Feng Z. 2002. Lake level and climate changes between 42,000 and 18,000 ^{14}C yr BP in the Tengger Desert, Northwestern China. *Quaternary Research* 58(1):62–72.
Zhang H, Peng J, Ma Y, Chen G, Feng Z-D, Li B, Fan H, Chang F, Lei G, Wünnemann B. 2004. Late Quaternary palaeolake levels in Tengger Desert, NW China. *Palaeogeography, Palaeoclimatology, Palaeoecology* 211(1–2):45–58.
Zhang H, Ming Q, Lei G, Zhang W, Fan H, Chang F, Wunnemann B, Hartmann K. 2006. Dilemma of dating on lacustrine deposits in an hyperarid inland basin of NW China. *Radiocarbon* 48(2):219–26.
Zhang J-F, Liu C-L, Wu X-H, Liu K-X, Zhou L-P. 2012. Optically stimulated luminescence and radiocarbon dating of sediments from Lop Nur (Lop Nor), China. *Quaternary Geochronology* 10:150–5.
Zhao Y, Yu Z, Chen F. 2009. Spatial and temporal patterns of Holocene vegetation and climate changes in arid and semi-arid China. *Quaternary International* 194(1):6–18.
Zhou A-F, Chen F-H, Wang Z-L, Yang M-L, Qiang M-R, Zhang J-W. 2011. Temporal change of radiocarbon reservoir effect in Sugan Lake, northwest China during the late Holocene. *Radiocarbon* 51(2):529–35.
Zhu L, Wu Y, Wang J, Lin X, Ju J, Xie M, Li M, Mäusbacher R, Schwalb A, Daut G. 2008. Environmental changes since 8.4 ka reflected in the lacustrine core sediments from Nam Co, central Tibetan Plateau, China. *The Holocene* 18(5):831–9.

APPENDIX

Definition and Notation of Carbon Isotope Species

The abundance of isotopic ratios $^{13}C/^{12}C$ and $^{14}C/^{12}C$ in the organic carbon of the atmospheric and catchment input can be expressed relative to that of a standard through a difference relationship known as the per mil notation

$$\delta^{13}C_a = \left[\left(\frac{^{13}C_a}{^{12}C_a} \right) \Big/ R_{PDB} - 1 \right] \times 1000 \quad \text{(A1)}$$

$$\delta^{13}C_c = \left[\left(\frac{^{13}C_c}{^{12}C_c} \right) \Big/ R_{PDB} - 1 \right] \times 1000 \quad \text{(A2)}$$

$$\delta^{13}C_c = \left[\left(\frac{^{13}C_c}{^{12}C_c} \right) \Big/ R_{PDB} - 1 \right] \times 1000 \quad \text{(A3)}$$

$$d^{14}C_c = \left[\left(\frac{^{14}C_c}{^{12}C_c} \right) \Big/ A_{ON} - 1 \right] \times 1000 \quad \text{(A4)}$$

where subscript *a* and *c* denote atmospheric and catchment input, respectively. R_{PDB} is the stable carbon isotopic molar ratio (i.e. $^{13}C/^{12}C$) of the Vienna Pee Dee Belemnite standard, and A_{ON} the radioactivity (i.e. $^{14}C/^{12}C$) of the oxalic acid standard normalized for isotope fractionation. Neglecting the radiogenic component (i.e. ^{14}C) that is usually present in trace amounts, the total molar mass of carbon isotope species in the organic carbon of atmospheric and catchment input can be expressed as

$$^{13}C_a + {}^{12}C_a = C_a \tag{A5}$$

$$^{13}C_c + {}^{12}C_c = C_c \tag{A6}$$

Rearranging Equations A1 and A2 gives the molar mass of $^{13}C_a$ and $^{13}C_c$

$$^{13}C_a = \left(\frac{\delta^{13}C_a}{1000} + 1\right) R_{PDB}\, {}^{12}C_a \tag{A7}$$

$$^{13}C_c = \left(\frac{\delta^{13}C_c}{1000} + 1\right) R_{PDB}\, {}^{12}C_c \tag{A8}$$

The fractionation abundance of $^{13}C_a$ and $^{13}C_c$ can be written as

$$F_a = \frac{^{13}C_a}{C_a} = \frac{^{13}C_a}{^{13}C_a + {}^{12}C_a} = \frac{\left(\frac{\delta^{13}C_a}{1000} + 1\right) R_{PDB}}{1 + \left(\frac{\delta^{13}C_a}{1000} + 1\right) R_{PDB}} \tag{A9}$$

$$F_c = \frac{^{13}C_c}{C_c} = \frac{^{13}C_c}{^{13}C_c + {}^{12}C_c} = \frac{\left(\frac{\delta^{13}C_c}{1000} + 1\right) R_{PDB}}{1 + \left(\frac{\delta^{13}C_c}{1000} + 1\right) R_{PDB}} \tag{A10}$$

Therefore, the molar mass of $^{12}C_a$ and $^{12}C_c$ can be expressed as

$$^{12}C_a = C_a\left(1 - F_a\right) = \frac{C_a}{1 + \left(\frac{\delta^{13}C_a}{1000} + 1\right) R_{PDB}} \tag{A11}$$

$$^{12}C_c = C_c\left(1 - F_c\right) = \frac{C_c}{1 + \left(\frac{\delta^{13}C_c}{1000} + 1\right) R_{PDB}} \tag{A12}$$

Similarly, rearranging Equations A3 and A4 gives the molar mass of $^{14}C_a$ and $^{14}C_c$

$$^{14}C_a = \left(\frac{d^{14}C_a}{1000} + 1\right) A_{ON}\, {}^{12}C_a = \frac{\left(\frac{d^{14}C_a}{1000} + 1\right) A_{ON} C_a}{1 + \left(\frac{\delta^{13}C_a}{1000} + 1\right) R_{PDB}} \tag{A13}$$

$$^{14}C_c = \left(\frac{d^{14}C_c}{1000} + 1\right) A_{ON}\, {}^{12}C_c = \frac{\left(\frac{d^{14}C_c}{1000} + 1\right) A_{ON} C_c}{1 + \left(\frac{\delta^{13}C_c}{1000} + 1\right) R_{PDB}} \tag{A14}$$

Linking d^{14}C to Percent Modern Carbon (pMC)

The radioactivity of organic carbon of the atmospheric and catchment input in terms of pMC is defined as (Stuiver and Polach 1977)

$$\mathrm{pMC_a} = \frac{A_{\mathrm{aN}}}{A_{\mathrm{ON}} e^{\lambda^*(y-1950)}} \times 100 \tag{A15}$$

$$\mathrm{pMC_c} = \frac{A_{\mathrm{cN}}}{A_{\mathrm{ON}} e^{\lambda^*(y-1950)}} \times 100 \tag{A16}$$

where $\lambda^* = 1/8267$ yr^{-1} is the ^{14}C decay constant based on the 5730-yr half-life, and y the year of measurements. A_{aN} and A_{cN} is the molar ratio of $^{14}C_a/^{12}C_a$ and $^{14}C_c/^{12}C_c$, respectively, normalized for isotope fractionation through (Stuiver and Polach 1977)

$$A_{\mathrm{aN}} = \frac{^{14}\mathrm{C_a}}{^{12}\mathrm{C_a}} \left[1 - \frac{2\left(25 + \delta^{13}\mathrm{C_a}\right)}{1000} \right] \tag{A17}$$

$$A_{\mathrm{cN}} = \frac{^{14}\mathrm{C_c}}{^{12}\mathrm{C_c}} \left[1 - \frac{2\left(25 + \delta^{13}\mathrm{C_c}\right)}{1000} \right] \tag{A18}$$

Substituting $^{12}C_a$, $^{12}C_c$, $^{14}C_a$, and $^{14}C_c$ with that given in the above section yields

$$A_{\mathrm{aN}} = \left(\frac{\mathrm{d}^{14}\mathrm{C_a}}{1000} + 1 \right) A_{\mathrm{ON}} \left[1 - \frac{2\left(25 + \delta^{13}\mathrm{C_a}\right)}{1000} \right] \tag{A19}$$

$$A_{\mathrm{cN}} = \left(\frac{\mathrm{d}^{14}\mathrm{C_c}}{1000} + 1 \right) A_{\mathrm{ON}} \left[1 - \frac{2\left(25 + \delta^{13}\mathrm{C_c}\right)}{1000} \right] \tag{A20}$$

Rearranging Equations A15 and A16 leads to

$$A_{\mathrm{aN}} = \frac{\mathrm{pMC_a}}{100} A_{\mathrm{ON}} e^{\lambda^*(y-1950)} \tag{A21}$$

$$A_{\mathrm{cN}} = \frac{\mathrm{pMC_c}}{100} A_{\mathrm{ON}} e^{\lambda^*(y-1950)} \tag{A22}$$

Equating Equations A19 and A21 and Equations A20 and A22, respectively, gives

$$\left(\frac{\mathrm{d}^{14}\mathrm{C_a}}{1000} + 1 \right) \left[1 - \frac{2\left(25 + \delta^{13}\mathrm{C_a}\right)}{1000} \right] = \frac{\mathrm{pMC_a}}{100} e^{\lambda^*(y-1950)} \tag{A23}$$

$$\left(\frac{\mathrm{d}^{14}\mathrm{C_c}}{1000} + 1 \right) \left[1 - \frac{2\left(25 + \delta^{13}\mathrm{C_c}\right)}{1000} \right] = \frac{\mathrm{pMC_c}}{100} e^{\lambda^*(y-1950)} \tag{A24}$$